Optical Modeling of MEMS Corner Cube Retroreflectors With Misalignment and Nonflatness

Xiaoming Zhu, *Student Member, IEEE*, Victor S. Hsu, and Joseph M. Kahn, *Fellow, IEEE*

***Abstract*—Micromachined corner cube retroreflectors (CCRs) can be employed as transmitters in free-space optical communication links. In this application, a CCR is illuminated by an unmodulated beam, and one mirror of the CCR is intentionally misaligned to modulate the intensity of the retroreflected beam. The low power consumption, small size, and ease of operation of a CCR makes it an attractive option for certain types of optical links. However, curvature and misalignment of the micromachined mirrors can cause CCRs to perform far from theoretical limits. In this paper, we develop two methods to predict the optical performance of CCRs having ideal or nonideal mirrors. We first introduce a discretized analysis method based on ray tracing and scalar diffraction theory. We then propose a simpler phase-shift model under the assumptions that the misalignment and surface nonflatness are small and that they do not alter the optical topology of the CCR. These assumptions are satisfied by typical CCRs to be used in free-space optical links. Using our two methods, we determine tolerances on mirror curvature and misalignment for representative micromachined CCRs.**

***Index Terms*—Free-space optical communications, MEMS CCR, misalignment, optical modeling, surface curvature.**

I. Introduction

A CORNER cube retroreflector (CCR) is a device made up of three mutually orthogonal reflective surfaces, or mirrors, forming a concave corner [1]–[3]. The mutual orthogonality ensures the light entering the CCR will be reflected back to the source, provided that it strikes the CCR within a region that depends on the direction of incidence. In Fig. 1, we illustrate the CCR's retroreflection property through ray tracing. By intermittently misaligning and realigning one or more of the CCR's mirrors, one can transmit a digitally modulated optical signal back to the interrogating light source. For example, in [1]–[3], two of the CCR's mirrors are fixed, while the third mirror is hinged and equipped with an electrostatic actuator, allowing the mirror to be tilted in response to an applied voltage. The hinged mirror-actuator system has a resonance frequency on the order of several kilohertz, allowing the CCR to transmit an optical signal at a bit rate up to several kilobits per second. The CCR has been proposed as a passive transmitter in a free-space optical communication system over a range of up to 1 km [4]. In this application, the CCR offers extremely low power consumption (<1 nJ/bit), ease of operation, and small size; CCRs under a cubic millimeter in size can be microfabricated in processes used for fabrication of microelectromechanical systems (MEMS). In practice, however, the performance of microfabricated CCRs can be degraded substantially by nonidealities, including nonflatness and misalignment of the mirrors. In this paper, we describe two methods of numerically computing the reflection characteristics of nonideal CCRs with misalignment and/or surface curvature. Using these techniques, one can determine specifications for CCR fabrication and predict the performance of free-space optical links using CCRs. Current optical MEMS processes can yield mirrors with surface roughness on the order of tens of nanometers. When these mirrors are illuminated in the visible or near-infrared range, surface roughness does not significantly impair CCR performance (see, e.g., [3]).

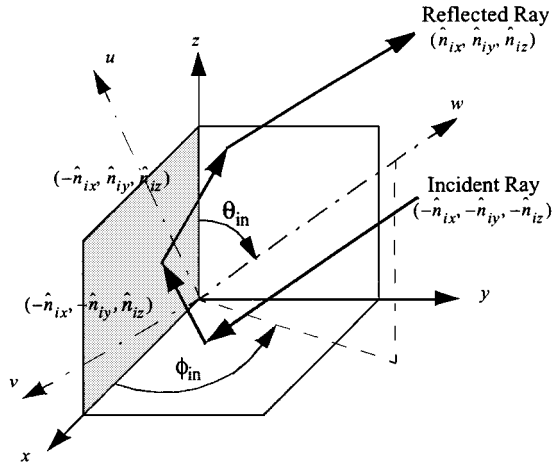

Fig. 1. Ray trace through an ideal CCR and the CCR coordinate system.

The remainder of this paper is organized as follows. In Section II, we introduce the geometrical optics description of CCRs. We define the characteristics of CCRs that are relevant for free-space optical communications, especially those determining the optical power reflected to the receiver. We then describe two methods for modeling the reflection characteristics of nonideal CCRs, including the discretized analysis method and the phase-shift method. In Section III, we apply these two methods to characterize the performance of CCRs having mirror curvature and misalignment. We present our conclusions in Section IV.

Manuscript received July 13, 2001; revised November 28, 2001. This work was supported by the DARPA MTO MEMS Program under Contract DABT63-98-1-0018.

The authors are with the Department of Electrical Engineering and Computer Sciences, University of California, Berkeley, CA 94720-1772 USA (e-mail: zhuxm@eecs.Berkeley.edu; vhsu@eecs.Berkeley.edu).

Publisher Item Identifier S 1077-260X(02)02221-9.

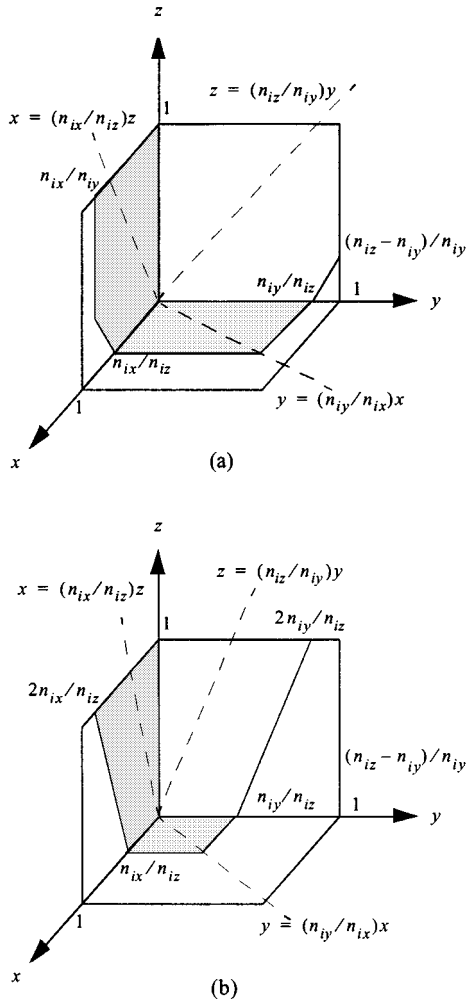

Fig. 2. Effective areas of CCR surfaces with incident direction $-\hat{n}_i$, where $\hat{n}_i = n_{ix}\hat{x} + n_{iy}\hat{y} + n_{iz}\hat{z}$ and $n_{iz} \geq n_{iy} \geq n_{ix}$. The two different cases are: (a) $2n_{iy} \geq n_{iz} \geq n_{iy} \geq n_{ix}$ and (b) $n_{iz} \geq 2n_{iy} \geq 2n_{ix}$.

II. Optical Modeling of MEMS CCR

A. Optical Characteristics of CCRs for Free-Space Optical Communication

Fig. 1 shows an ideal CCR and defines the *CCR coordinate system* (x, y, z). In an ideal CCR, the mirrors are normal to the x, y, and z axes, respectively. An incident ray strikes the CCR along the *incidence direction* $-\hat{n}_i$, where $\hat{n}_i = n_{ix}\hat{x} + n_{iy}\hat{y} + n_{iz}\hat{z}$, i.e., $\hat{n}_i = (n_{ix}, n_{iy}, n_{iz})$, with $n_{ix}^2 + n_{iy}^2 + n_{iz}^2 = 1$. The ray undergoes three reflections, each reflection changing the ray's direction along one of the coordinates, so that the reflected ray exits the CCR along the direction $\hat{n}_i$.[1] Not all rays that strike the CCR will be reflected back to the light source, however. Whether a given ray is reflected back depends on both the incident direction $-\hat{n}_i$ and on where the ray first strikes the CCR. For a given $\hat{n}_i$, we define the effective area on a mirror's surface such that an incident ray first striking the mirror within the effective area will be reflected back to the source. The effective area can be determined by ray tracing. Because of the symmetry of an ideal CCR, it is sufficient to consider the case that $n_{iz} \geq n_{iy} \geq n_{ix}$. In Fig. 2, we depict the effective area in each of the two possible cases, i.e., $2n_{iy} \geq n_{iz} \geq n_{iy} \geq n_{ix}$ and $n_{iz} \geq 2n_{iy} \geq 2n_{ix}$. For other incident directions, we can determine the effective area by permuting the x, y, and z coordinates in Fig. 2. In Fig. 2, each mirror's effective area is divided by a dashed line into two subareas. If an incident ray strikes the CCR in a given subarea of one mirror, upon reflection, the beam will strike the mirror adjacent to that subarea. All rays incident upon a given subarea will reflect off the three mirrors in the same order. Since a ray trace is reversible, all rays exiting the CCR from a given subarea will have reflected off the three mirrors in the same order.

[1]There also exist two boundary cases, in which an incident ray can strike only one or two mirrors and be returned to the source. The single-reflection case occurs when an incident ray is normal to a mirror, while the double-reflection case occurs when an incident ray is parallel to one mirror surface and not normal to either of the other mirrors. In typical communications applications, CCRs are randomly oriented, and each of the boundary cases occurs with zero probability. Hence, in this paper, we restrict our attention to the three-reflection case.

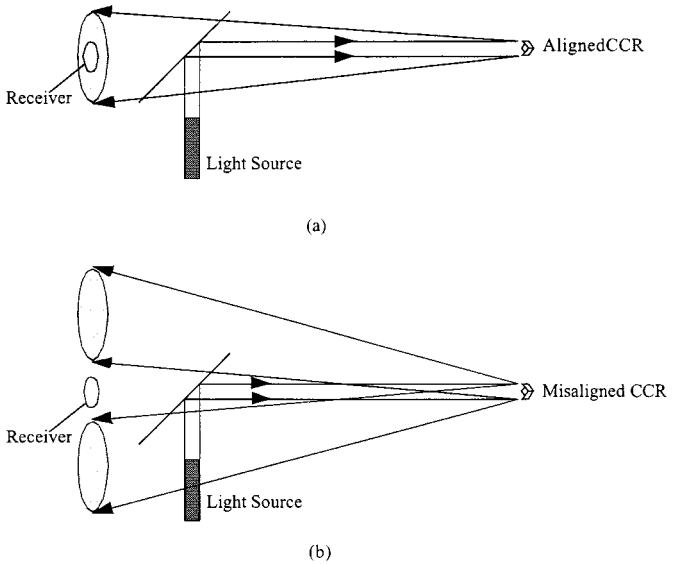

Fig. 3. On–off-keyed free-space optical link using a CCR: (a) on state and (b) off state.

For each given $\hat{n}_i$, we define a light-path coordinate system (u, v, w), where the w-axis is along the direction of $\hat{n}_i$. As shown in Fig. 1, in the CCR coordinate system (x, y, z), we can represent $\hat{n}_i$ in spherical coordinates as $(\rho, \theta_{in}, \varphi_{in})$, with $\rho = 1$. Hence, the transformation between the CCR coordinate system (x, y, z) and the light-path coordinate system (u, v, w) is given by

$$\begin{bmatrix} u \\ v \\ w \end{bmatrix} = \begin{bmatrix} \cos\varphi_{in} \cdot \cos\theta_{in} & \sin\varphi_{in} \cdot \cos\theta_{in} & \sin\theta_{in} \\ -\sin\varphi_{in} & \cos\varphi_{in} & 0 \\ -\cos\varphi_{in}\sin\theta_{in} & -\sin\varphi_{in} & \cos\theta_{in} \end{bmatrix} \begin{bmatrix} x \\ y \\ z \end{bmatrix}. \tag{1}$$

We project the effective areas of all three mirrors onto the u–v plane, and we define the sum of the projected effective areas to be the total effective area. For each incidence direction $-\hat{n}_i$, we can consider the CCR output beam to be reflected from a single flat mirror perpendicular to $\hat{n}_i$ and having an area equal to the total effective area and a reflectance equal to r_m^3, where each individual mirror has reflectance r_m.

In a free-space optical link, the CCR is illuminated along $-\hat{n}_i$ and the reflected light is monitored by a receiver along the observation direction $\hat{n}_o = \hat{n}_i$, as depicted in Fig. 3. When the

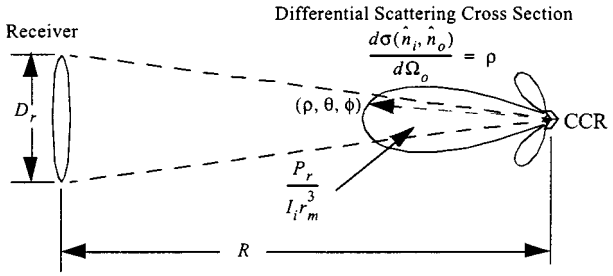

Fig. 4. Calculating the power received by a receiver from a CCR. The DSCS profile is shown in a spherical coordinate system. The angular coordinates (θ, ϕ) of the spherical coordinate represents the direction of $\hat{n}_o$, and the radial coordinate ρ denotes the DSCS $d\sigma(\hat{n}_i, \hat{n}_o)/d\Omega_o = \rho$.

three CCR mirrors are mutually perpendicular, the CCR is in the on state, and reflects light to the receiver, as in Fig. 3(a). When one of the mirrors is misaligned by a sufficiently large angle δ, the CCR is in the off state, and rays exiting the CCR will be directed away from the receiver, as in Fig. 3(b). Thus, by mechanically actuating one of the CCR mirrors, we can transmit an on–off-keyed (OOK) signal.

In this paper, we focus on the characteristics of CCRs that determine the power received in a free-space optical link. We make reference to Fig. 4. Assume that the CCR is illuminated along the direction $-\hat{n}_i$ by an irradiance I_i (measured at the CCR). Suppose that the reflected light is observed along the direction $\hat{n}_o$ by a receiver subtending a solid angle Ω_r at the CCR. The CCR's light-reflecting properties are characterized by the differential scattering cross section (DSCS) $d\sigma(\hat{n}_i, \hat{n}_o)/d\Omega_o$, which is the reflected power per unit solid angle of observation per unit illumination irradiance. The DSCS is a function of the incident direction $-\hat{n}_i$ and the observation direction $\hat{n}_o$ and has units (W/sr)/(W/m^2), i.e., m^2/sr. In terms of the DSCS, the received power P_r is given by

$$P_r = I_i r_m^3 \int_{\Omega_o \in \Omega_r} \frac{d\sigma(\hat{n}_i, \hat{n}_o)}{d\Omega_o} \, d\Omega_o. \tag{2}$$

The solid angle subtended by the receiver can be computed using

$$\Omega_r = 2\pi \left(1 - \frac{R}{\sqrt{R^2 + \frac{D_r^2}{4}}} \right) \tag{3}$$

where D_r is the receiver diameter and R is the distance from the CCR to the receiver. Note that for a given $\hat{n}_i$, the integral of $d\sigma(\hat{n}_i, \hat{n}_o)/d\Omega_o$ over all Ω_o equals the total effective area.

The colinear differential scattering cross section (CDSCS) is defined as the value of $d\sigma(\hat{n}_i, \hat{n}_o)/d\Omega_o$ when the axes of illumination and observation are colinear $\hat{n}_o = \hat{n}_i$. The CDSCS is relevant because in practice the receiver is almost always placed along the axis of illumination, and the distance R is much larger than the receiver diameter D_r. Hence, the receiver subtends a small solid angle, over which the DSCS is approximately equal to the CDSCS. Therefore, the power received can be calculated approximately as follows:

$$P_r \approx I_i r_m^3 \cdot \frac{d\sigma(\hat{n}_i, \hat{n}_i)}{d\Omega_o} \cdot \Omega_r. \tag{4}$$

In many applications [4], the CCRs are randomly oriented with respect to the direction of the light source/receiver. A useful parameter describing the performance of free-space links using randomly oriented CCRs is the complementary cumulative distribution function (CCDF) of the CDSCS normalized to the CDSCS along the body diagonal $(\hat{n}_i = 1/\sqrt{3}(1, 1, 1))$

$$\text{CCDF}(x) = \text{Prob}\left[\frac{d\sigma((\hat{n}_i, \hat{n}_o = \hat{n}_i)/d\Omega_o)}{d\sigma\left(\hat{n}_i = \frac{1}{\sqrt{3}}(1, 1, 1), \hat{n}_o = \hat{n}_i\right)\Big/ d\Omega_o} > x \right] \tag{5}$$

where x is the normalized CDSCS. Suppose that in order to receive properly from a CCR, it is required that the CDSCS be some specified fraction x_0 of the CDSCS along the body diagonal. Then CCDF(x_0) is the probability that one can receive from a randomly oriented CCR. In this paper, we assume that the CCRs are randomly oriented over an entire unit sphere. In some applications, the CCRs may be oriented randomly over a half-sphere [4].

B. Calculating the DSCS of Nonideal CCRs

In this section, we describe how to calculate the DSCS of nonideal CCRs, in which the mirrors may have curvature and/or misalignment. First, we introduce a discretized analysis method that combines ray tracing and diffraction theory. While generally applicable, this method requires lengthy computations. We then describe a phase-shift model, which greatly simplifies the computation. The phase-shift model is valid as long as any curvature and misalignment of the CCR is small enough that the CCR optical topology can be considered to remain unchanged. This assumption must usually be satisfied by CCRs in order to achieve satisfactory performance.

1) Discretized Analysis: To begin the analysis, the surface of each CCR mirror is described by an equation. The CCR faces are bounded by the planes $x = 0$, $x = 1$, $y = 0$, $y = 1$, $z = 0$, and $z = 1$, as in Fig. 1, where each axis is normalized by the lengths that each mirror would have if the three were perfectly flat and mutually perpendicular. In practice, the surfaces are sufficiently close to flat and orthogonal that the error introduced by not adjusting the boundary conditions is negligible. Each surface is divided into a specified number of discrete elements that are bounded by equally spaced planes parallel to the x–y, y–z, and x–z planes. In Fig. 5(a), we show an example of dividing one surface into four discrete elements. If the surfaces were perfectly flat, these discrete elements would be squares of equal size. For nonflat surfaces, the different discrete elements have various surface areas and shapes. We choose the number of discrete elements to be sufficiently large so that we can approximate each surface as flat. The normal vector of each discrete element is determined by computing the Jacobian of the equation describing the surface, evaluated at the center of the element.

Fig. 5(b) depicts the analysis of a single discrete element of the CCR. We assume that the CCR is illuminated along the direction $-\hat{n}_i$ by a uniform plane wave having an irradiance I_i.

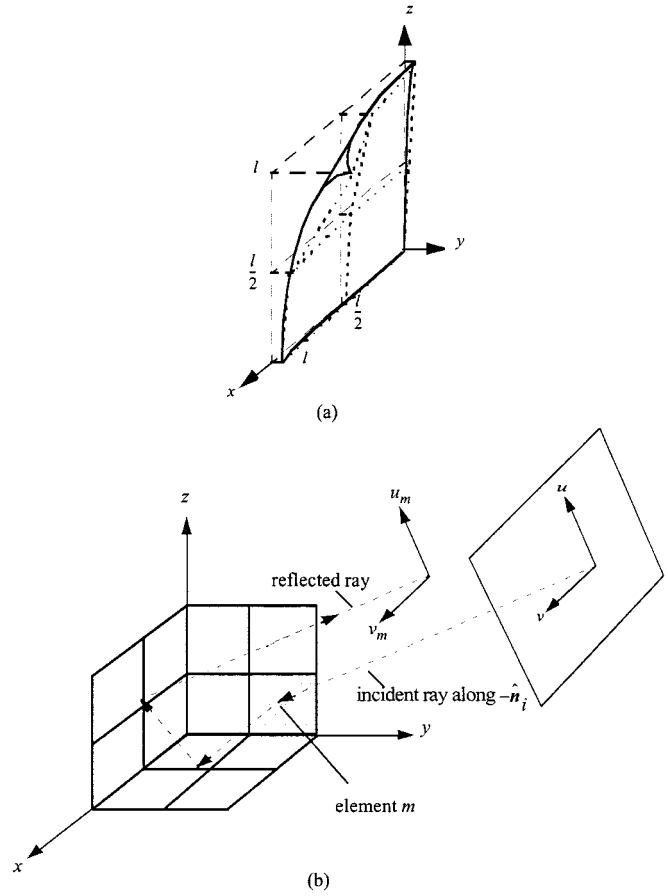

Fig. 5. (a) Discretization of the CCR surfaces. (b) Analysis of element m in the CCR.

This is a good approximation for free-space optical communication over a few hundred meters or longer with CCRs of submillimeter scale. For each discrete element m, a ray trace is performed to determine the direction of the ray leaving the CCR. The ray starts from a reference plane in which all rays striking the CCR are in phase. This reference plane is normal to the incident direction $\hat{n}_i$ and passes through an arbitrary point near the CCR, i.e., parallel to the u–v plane in the light-path coordinate system. After the ray strikes discrete element m, the direction of the reflected ray can be determined from the incidence vector and the normal vector of element m. The next surface that the ray strikes, if any, is then determined, and the ray trace continues. Finally, the ray exits the CCR and is terminated on a second reference plane, the u_m–v_m plane, which is defined by two arbitrary unit vectors, u_m and v_m, which are perpendicular to the exiting ray and to each other. The u_m–v_m plane for each discrete element m can be chosen to pass through an arbitrarily chosen point near the CCR (possibly different for each m). Unlike the u–v plane, each u_m–v_m plane is unique to a discrete element m unless the three mirrors are perfectly flat.

It is also important to keep track of the distance d_m that each ray propagates through the ray trace and the number of reflections $N_{\mathrm{ref,\,m}}$ that each ray undergoes. These values are needed to specify the phase change and the transverse extent of the wave reflected from the discrete element.

In order to treat diffraction effects, we employ the Fraunhofer diffraction theory [5], which is valid when the receiver lies in the far field. More precisely, this requires that $R > a^2/\lambda$, where R is the distance from the aperture to the receiver, a is the largest dimension of the output aperture, and λ is the wavelength of the light. For most free-space optical communication systems, the transmission distance is large enough to satisfy the far-field condition. The complex electric field amplitude contributed by discrete element m at the observation point P is given by

$$E_m(\hat{n}_i, \hat{n}_o, R) = \frac{\sqrt{2I}_i e^{-i(kd_m + \pi N_{\mathrm{ref,\,m}})}}{\lambda R} \cdot \iint_{S_m} e^{-ikR_P(u_m, v_m)}\, du_m\, dv_m \quad (6)$$

where $k = 2\pi/\lambda$. In (6), S_m is the projected area of the mth discrete element on its u_m–v_m plane, and $R_P(u_m, v_m)$ is the distance between (u_m, v_m) on S_m and the receiver position P.

The sum over all discrete elements gives the complex amplitude of the total electric field at the receiver

$$E_o(\hat{n}_i, \hat{n}_o, R) = \sum_m E_m(\hat{n}_i, \hat{n}_o, R). \quad (7)$$

The irradiance at the receiver can be calculated from this total electric field using

$$I_o(\hat{n}_i, \hat{n}_o, R) = \tfrac{1}{2}|E_o(\hat{n}_i, \hat{n}_o, R)|^2. \quad (8)$$

The differential scattering cross section (DSCS) $d\sigma(\hat{n}_i, \hat{n}_o)/d\Omega_o$ (m^2/sr) can be calculated from the irradiance using

$$\frac{d\sigma(\hat{n}_i, \hat{n}_o)}{d\Omega_o} = \frac{I_o R^2}{I_i}. \quad (9)$$

The integral of the differential scattering cross section over all observation angles equals the total scattering cross section of the CCR, $\sigma(\hat{\boldsymbol{n}}_i)$, which has units of m^2

$$\int_{4\pi} \frac{d\sigma(\hat{\boldsymbol{n}}_i, \hat{\boldsymbol{n}}_o)}{d\Omega_o}\, d\Omega_o = \sigma(\hat{\boldsymbol{n}}_i). \quad (10)$$

2) Phase-Shift Model: In order for CCRs to perform well in free-space links, mirror misalignment and nonflatness must be small. In the phase-shift model, we assume that these effects are sufficiently weak that the geometrical optical topology of the CCR can be assumed to remain ideal, as depicted in Figs. 1 and 2. Under this assumption, all u_m–v_m planes lie parallel to the u–v plane, and so all u_m–v_m planes can be chosen to coincide with the u–v plane. As in Fig. 5(a), the light exiting from the CCR can be assumed to be exiting from the total effective area on the u–v plane. We account for the effects of mirror misalignment and nonflatness by introducing corresponding phase shifts to the light rays exiting the CCR. The details are given as follows.

We model nonflat mirrors as spherical surfaces, following previous work [1], [6] showing that this is a good model for representative nonflat MEMS mirrors. For nonflat mirrors, we characterize mirror alignment by considering a vector normal to each mirror at the mirror's center. The CCR is considered to be misaligned when any of these normal vectors deviates from the ideal CCR coordinate system, as shown in Fig. 1. Knowing the incidence direction of a ray, the normal vector to a CCR mirror

surface (at the center of the mirror), and the mirror radius of curvature, we can compute the phase delay of the ray as compared to the ideal CCR. For example, assuming that for the mirror in the x–y plane, the normal vector is

$$\hat{n}_{xy} = \frac{1}{\sqrt{(\delta_x^z)^2 + (\delta_y^z)^2 + 1}} (\delta_x^z, \delta_y^z, 1)$$

and the radius of curvature is R_{xy}, the phase delay at position (x, y) is

$$\delta\varphi_{xy}(x, y) = 2k \cos[\theta(\hat{n}_{xy}, \hat{n}_i)] \cdot (\Delta_{xy}^m + \Delta_{xy}^c) \quad (11)$$

where

$$\Delta_{xy}^m = x\delta_x^z + y\delta_y^z$$
$$\Delta_{xy}^c = \sqrt{R_{xy}^2 - \left(x - \frac{l}{2}\right)^2 - \left(y - \frac{l}{2}\right)^2} - R_{xy} \quad (12)$$

and where $\theta(\hat{n}_{xy}, \hat{n}_i)$ is the angle between the vectors $\hat{n}_{xy}$ and $\hat{n}_i$.

Under the assumptions made here, we can assume that in a nonideal CCR, each ray follows a path topologically equivalent to the path through an ideal CCR. For each ray exiting from the total effective area at (u, v), we can trace backward through an ideal CCR to find the positions at each mirror surface where the ray has been reflected. The total phase delay of a ray exiting at (u, v) (as compared to an ideal CCR) is the sum of the phase delays caused by reflections from the three nonideal mirrors

$$\delta\varphi_{uv}(u, v) = \delta\varphi_{xy}(x, y) + \delta\varphi_{xy}(y, z) + \delta\varphi_{xy}(z, x). \quad (13)$$

The complex electric field amplitude at the receiver position P is given by

$$E_o(\hat{n}_i, \hat{n}_o, R) = \frac{\sqrt{2I}_i e^{-i(kd + \pi N_{\text{rcf}})}}{\lambda R} \cdot \iint_{S_{uv}} e^{-i[kR_P(u,v) + \delta\varphi_{uv}(u,v)]} \, du \, dv \quad (14)$$

where S_{uv} is the total effective area at the u–v plane. Using (8), (9), and (14), we can compute the DSCS of a CCR much more easily than using discretized analysis.

III. Results and Discussion

In this section, we apply the optical models described above to investigate the influence of misalignment and surface nonflatness on CCR optical characteristics that affect free-space links. In all of the following, we assume that the illuminating light has a wavelength $\lambda = 529$ nm and that all three CCR mirrors are squares of equal size. When considering nonflat mirrors, all three mirrors are assumed to be spherical with equal radius of curvature R_c.

We first consider a CCR having flat mirrors, with one mirror misaligned by an angle δ, as shown in Fig. 6(a). Each mirror is 250 μm square. We consider incidence directions $\hat{n}_i = 1/\sqrt{3}(1, 1, 1)$ and $1/\sqrt{2.3}(0.7, 0.9, 1)$. In Fig. 6(b), we show the CDSCS versus misalignment angle δ, computed using both discretized analysis and the phase-shift model. Results calculated using the two methods are seen to agree closely. Fig. 6(b) shows that when the CCR is perfectly aligned, the CDSCS for $\hat{n}_i = 1/\sqrt{3}(1, 1, 1)$ is larger than

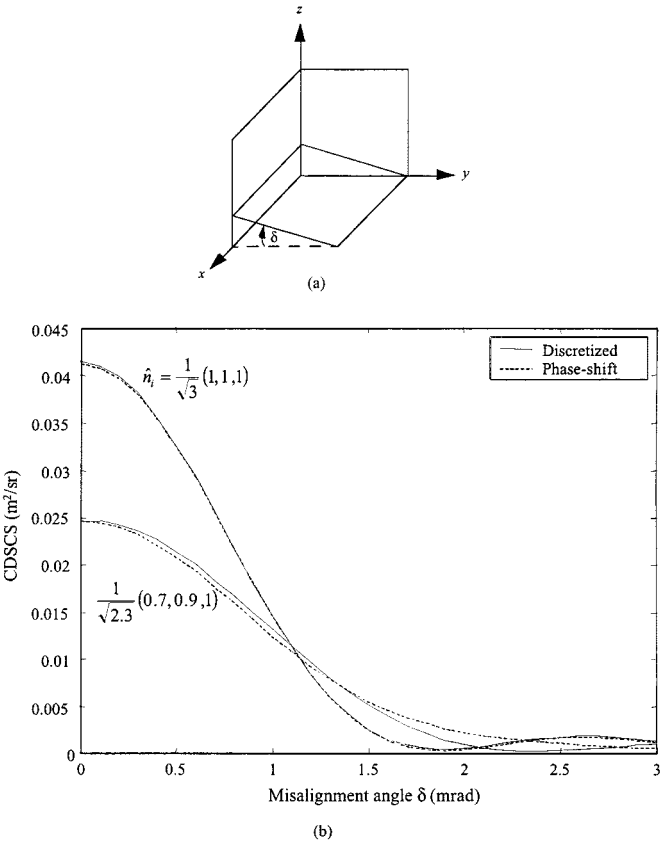

Fig. 6. (a) Misalignment of one of the CCR mirrors by an angle δ. (b) CDSCS versus the misalignment angle δ computed using both discretized analysis and the phase-shift model. Each CCR mirror is 250 μm square, and the incident directions $\hat{n}_i$ are $1/\sqrt{3}(1, 1, 1)$ and $1/\sqrt{2.3}(0.7, 0.9, 1)$, respectively.

that for $\hat{n}_i = 1/\sqrt{2.3}(0.7, 0.9, 1)$ because the total effective area is larger for the former incidence direction. When one mirror is misaligned, however, the CDSCS degrades more rapidly for the former incidence direction because misalignment induces larger phase variations over the larger effective area. In Fig. 6(b), we observe that when $\delta > 1.2$ mrad, the CDSCS for $\hat{n}_i = 1/\sqrt{3}(1, 1, 1)$ actually falls below that for $\hat{n}_i = 1/\sqrt{2.3}(0.7, 0.9, 1)$. In Fig. 6(b), we see that a misalignment angle of only 2 or 3 mrad is sufficient to switch this CCR from the on state to the off state.

We have performed additional calculations (not shown here) comparing the discretized method and the phase-shift model, which have verified the accuracy of the latter technique. In the remainder of this paper, we employ the phase-shift model to study the effects of mirror nonflatness and misalignment on CCR performance.

Depending on the fabrication process, MEMS mirrors may be subject to varying degrees of nonflatness. In Fig. 7, we plot the CDSCS versus mirror size for radii of curvature $R_c = \infty$, 1, 0.5, and 0.2 m. We consider incidence directions $\hat{n}_i = 1/\sqrt{3}(1, 1, 1)$ and $1/\sqrt{2.3}(0.7, 0.9, 1)$. We see that when the radius of curvature R_c is large, the CDSCS increases rapidly with increasing mirror size (i.e., with increasing effective area) for both incidence directions. When R_c is small, however, the CDSCS increases less rapidly with increasing mirror size. In fact, when $R_c = 0.2$ m or smaller, increasing the mirror size fails to increase the CDSCS and may even decrease

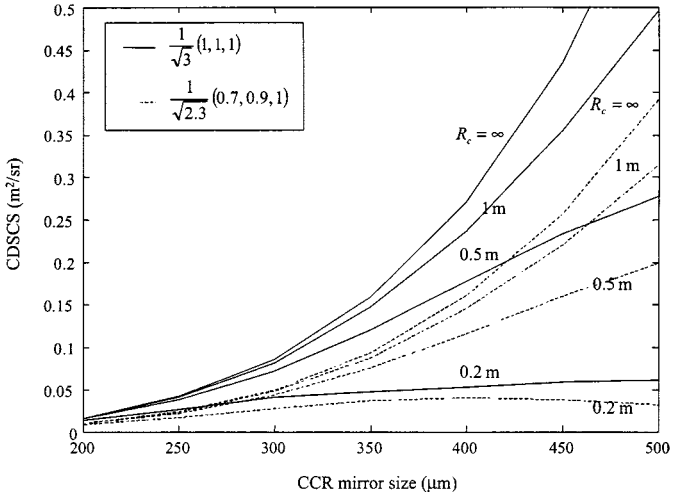

Fig. 7. CDSCS versus the CCR mirror size computed by the phase-shift model. All three mirrors have radii of curvature R_c, where R_c takes on the values ∞, 1, 0.5 and 0.2 m, respectively. The incident directions $\hat{n}_i$ are $1/\sqrt{3}(1, 1, 1)$ (solid line) and $1/\sqrt{2.3}(0.7, 0.9, 1)$ (dashed line), respectively.

the CDSCS; this is because increasing the mirror size leads to increased optical phase variation over the increased effective area. The data in Fig. 7 clearly illustrate the importance of mirror flatness in achieving good CCR performance.

We now consider the combined effects of mirror misalignment and nonflatness. As before, we choose incidence directions $\hat{n}_i = 1/\sqrt{3}(1, 1, 1)$ and $1/\sqrt{2.3}(0.7, 0.9, 1)$. In Fig. 8, we plot the CDSCS versus the misalignment angle δ for radii of curvature $R_c = 1$, 0.5, and 0.2 m. We choose the mirror sizes to be 250 and 400 μm, respectively, in Fig. 8(a) and (b). The data in Fig. 8 show that the CDSCS degrades with both increasing δ and decreasing R_c. Our calculations have shown that for large R_c, to achieve a CDSCS close to the optimal value, the tolerable δ is approximately inversely proportional to the mirror size. For smaller values of R_c, the effect of misalignment angle δ is reduced, because at least some portion of the curved mirror surface remains relatively well aligned.

In Fig. 9, we present the effects of misalignment and curvature on the CCDF of the CDSCS normalized to its value when the incidence direction lies along the body diagonal, $\hat{n}_i = 1/\sqrt{3}(1, 1, 1)$. The mirror sizes are chosen to be 250 and 400 μm in Fig. 9(a) and (b), respectively. In each figure, we consider a perfect CCR, a CCR having one mirror misaligned at $\delta = 0.6$ mrad, a CCR having radii of curvature $R_c = 20$ cm, and a CCR having both misalignment and curvature. As we see in Fig. 9(a), when the mirror size is 250 μm, the misalignment alone causes little change in the CCDF. The curvature alone causes a noticeable increase in the CCDF, especially for relatively high values of the normalized CDSCS. The combined misalignment and curvature lead to a more noticeable increase in the CCDF for all but the smallest values of the normalized CDSCS. These increases of the CCDF occur because curvature or combined misalignment and curvature tend to degrade the CDSCS most significantly for incidence directions for which the total effective area is largest, such as along the body diagonal. Since the CDSCS along the body diagonal is the normalization factor in the CCDFs shown in

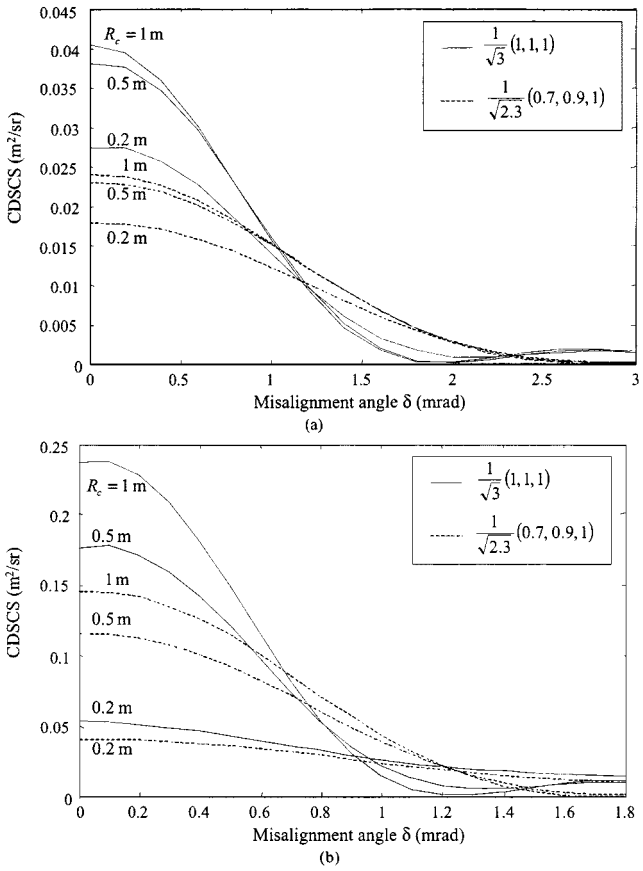

Fig. 8. CDSCS versus the misalignment angle δ [as defined in Fig. 6(a)] for different CCR mirror radii of curvature computed by the phase-shift model. The CCR mirror sizes are: (a) 250 and (b) 400 μm. All three mirrors have radii of curvature R_c, where R_c takes on the values 1, 0.5, and 0.2 m respectively. The incident directions $\hat{n}_i$ are $1/\sqrt{3}(1, 1, 1)$ (solid line) and $1/\sqrt{2.3}(0.7, 0.9, 1)$ (dashed line), respectively.

Fig. 9, these nonidealities can increase the CCDFs. When we increase the mirror size to 400 μm, as in Fig. 9(b), all the effects described above become even more pronounced. In Fig. 9(b), the CCDF with combined misalignment and curvature does not go to zero for $x = 1$ because under these conditions, the CDSCS is not largest for incidence directions along the body diagonal but is actually largest for other nearby incidence directions. The results shown in Fig. 9 can be used to compute the probability that in a free-space communication system, a randomly oriented CCR will reflect sufficient light back to the receiver.

IV. Conclusion

Micromachined CCRs can be used to transmit data in free-space optical communication systems. However, their performance can be far from theoretical limits because of misalignment and the nonflatness of the mirrors. In this paper, we have defined certain parameters to describe the optical characteristics of CCRs for data transmission, such as DSCS, CDSCS, and CCDF. We then developed optical models to compute these parameters. These optical models can be used to predict the performance of CCRs, determine device fabrication tolerances, and optimize device specifications.

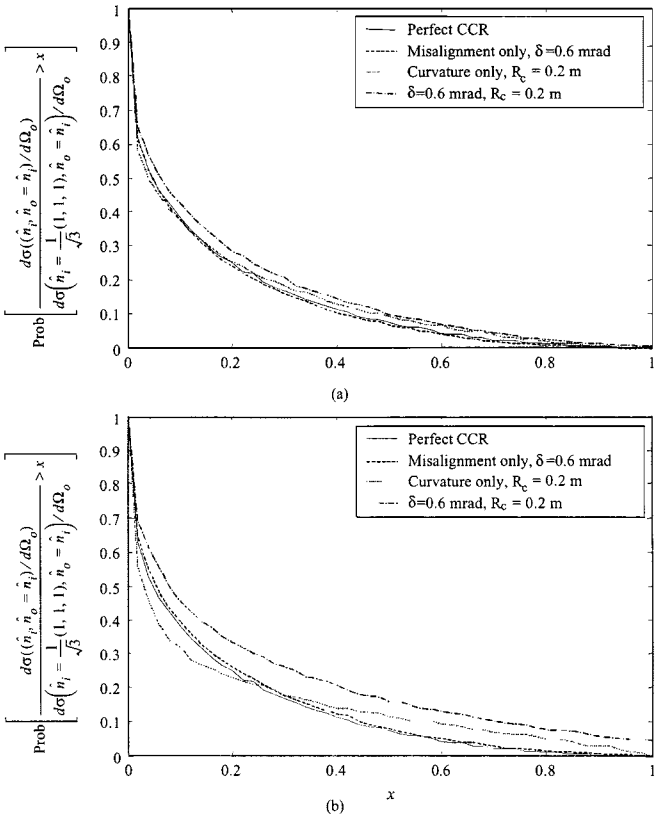

Fig. 9. Complementary cumulative distribution function of normalized CDSCS $[d\sigma(\hat{n}_i, \hat{n}_o = \hat{n}_i)/d\Omega_0]/[d\sigma(\hat{n}_i = 1/\sqrt{3}(1, 1, 1), \hat{n}_o = \hat{n}_i)/d\Omega_0]$ for CCRs with mirror sizes: (a) 250 and (b) 400 μm, respectively, computed using the phase-shift model. The cases of perfect CCR (solid line), CCR with one surface misaligned with $\delta = 0.6$ mrad (dashed line), CCR with radius of curvature 20 cm (dotted line), and CCR with both misalignment and radius of curvature (dash-dot line) are shown for comparison.

ACKNOWLEDGMENT

The authors are grateful for discussions with K. Pister and L. Zhou.

REFERENCES

[1] V. S. Hsu, "MEMS corner cube retroreflectors for free-space optical communications," Masters dissertation, EECS Dept., Univ. California, Berkeley, Berkeley, CA, Oct. 1999.

[2] P. B. Chu, N. R. Lo, E. C. Berg, and K. S. J. Pister, "Optical communication using micro corner cube reflectors," in *Proc. IEEE Microelectromechanical Systems Workshop*, Nagoya, Japan, 1997, pp. 350–355.

[3] L. Zhou, K. S. J. Pister, and J. M. Kahn, "Assembled corner-cube retroreflector quadruplet," in *15th IEEE Int. Conf. Microelectromechechanical Systems*, Las Vegas, NV, Jan. 20–24, 2002.

[4] J. M. Kahn, R. H. Katz, and K. S. J. Pister, "Next century challenges: Mobile networking for smart dust," in *Proc. ACM/IEEE Int. Conf. Mobile Computing and Networking (MobiCom 99)*, Seattle, WA, Aug. 17–19, 1999, pp. 271–278.

[5] M. Born and E. Wolf, *Principles of Optics*, 7th ed. Cambridge, U.K.: Cambridge Univ. Press, 1999.

[6] J. E. Ford, V. A. Aksyuk, D. J. Bishop, and J. A. Walker, "Wavelength add-drop switching using tilting micromirrors," *J. Lightwave Technol.*, vol. 17, pp. 904–911, May 1999.

Xiaoming Zhu (S'02) was born in 1974 and received the B.S. degree from Tsinghua University, Beijing, China in 1997. He is currently working towards the Ph.D. in the Department of Electrical Engineering and Computer Sciences at University of California, Berkeley.

His research interests include wireless communication, free-space optical communication, and optical fiber communication networks.

Victor S. Hsu received the B.S. degree in electrical engineering from the University of Illinois, Urbana-Champaign, in 1997, and the M.S. degree in electrical engineering from the University of California, Berkeley, in 1999.

At the University of California, Berkeley, he conducted research on wireless free-space optical communications with MEMS corner cube retroreflectors.

Joseph M. Kahn (M'90–SM'98–F'00) received the A.B., M.A., and Ph.D. degrees in physics from University of California, Berkeley, in 1981, 1983, and 1986, respectively.

He is a Professor in the Department of Electrical Engineering and Computer Sciences at University of California, Berkeley. In 2000, he co-founded StrataLight Communications, Inc., where he is currently Chief Scientist. From 1987 to 1990 he was a Member of Technical Staff in the Lightwave Communications Research Department of AT&T Bell Laboratories, where he performed research on multigigabit-per-second coherent optical fiber transmission systems, setting several world records for receiver sensitivity. He joined the faculty of University of California, Berkeley in 1990. His current research interests include wireless communication using antenna arrays, free-space optical communication, optical fiber communication, and wireless communication for networks of sensors based on micro-electromechanical systems.

Dr. Kahn received the National Science Foundation Presidential Young Investigator Award in 1991. From 1993 to 2000, he served as a technical editor of *IEEE Personal Communications Magazine*.